

AD-A092376

AD A092376
TECHNICAL
LIBRARY

AD

TECHNICAL REPORT ARBRL-TR-02262

FRANCK-CONDON FACTORS FOR THE
B-X SYSTEM OF S_2

William R. Anderson
John E. Allen, Jr.
David R. Crosley

August 1980



US ARMY ARMAMENT RESEARCH AND DEVELOPMENT COMMAND
BALLISTIC RESEARCH LABORATORY
ABERDEEN PROVING GROUND, MARYLAND

Approved for public release; distribution unlimited.

Destroy this report when it is no longer needed.
Do not return it to the originator.

Secondary distribution of this report by originating
or sponsoring activity is prohibited.

Additional copies of this report may be obtained
from the National Technical Information Service,
U.S. Department of Commerce, Springfield, Virginia
22151.

The findings in this report are not to be construed as
an official Department of the Army position, unless
so designated by other authorized documents.

*The use of trade names or manufacturers' names in this report
does not constitute indorsement of any commercial product.*

UNCLASSIFIED

SECURITY CLASSIFICATION OF THIS PAGE (When Data Entered)

REPORT DOCUMENTATION PAGE		READ INSTRUCTIONS BEFORE COMPLETING FORM
1. REPORT NUMBER TECHNICAL REPORT ARBRL-TR-02262	2. GOVT ACCESSION NO.	3. RECIPIENT'S CATALOG NUMBER
4. TITLE (and Subtitle) FRANCK-CONDON FACTORS FOR THE B-X SYSTEM OF S ₂		5. TYPE OF REPORT & PERIOD COVERED BRL Technical Report
7. AUTHOR(s) William R. Anderson John E. Allen, Jr. * David R. Crosley**		6. PERFORMING ORG. REPORT NUMBER
9. PERFORMING ORGANIZATION NAME AND ADDRESS US Army Armament Research and Development Command US Army Ballistic Research Laboratory ATTN: DRDAR-BL Aberdeen Proving Ground, MD 21005		8. CONTRACT OR GRANT NUMBER(s)
11. CONTROLLING OFFICE NAME AND ADDRESS US Army Armament Research & Development Command US Army Ballistic Research Laboratory ATTN: DRDAR-BLP Aberdeen Proving Ground, MD 21005		10. PROGRAM ELEMENT, PROJECT, TASK AREA & WORK UNIT NUMBERS 1L161102AH43
14. MONITORING AGENCY NAME & ADDRESS (if different from Controlling Office)		12. REPORT DATE AUGUST 1980
		13. NUMBER OF PAGES 44
		15. SECURITY CLASS. (of this report) Unclassified
		15a. DECLASSIFICATION/DOWNGRADING SCHEDULE
16. DISTRIBUTION STATEMENT (of this Report) Approved for public release; distribution unlimited.		
17. DISTRIBUTION STATEMENT (of the abstract entered in Block 20, if different from Report)		
18. SUPPLEMENTARY NOTES *NAS-NRC Resident Research Associate; Present address: Goddard Space Flight Center, Greenbelt, MD 20770 **Present address: Molecular Physics Laboratory, SRI International, Menlo Park, CA 94025		
19. KEY WORDS (Continue on reverse side if necessary and identify by block number) Laser Excited Fluorescence Franck-Condon Factors Intensities Diatomic Sulfur		
20. ABSTRACT (Continue on reverse side if necessary and identify by block number) (clt) A frequency doubled tunable dye laser has been used to selectively excite individual vibrational levels within v=2 and 6-9 of the B-state of diatomic sulfur. Measurements of the intensity in emission of all the terms returning to ground state vibrational levels permit the determination of absolute Franck- Condon factors. Combined with previous studies, this work completes the set of Franck-Condon factors for bound-bound transitions within the B-X system. (see reverse side)		

UNCLASSIFIED

SECURITY CLASSIFICATION OF THIS PAGE(When Data Entered)

20. ABSTRACT (Cont'd)

A simple pictorial representation of the Franck-Condon factors is presented and conclusions may be drawn concerning the overlap with the B-state wavefunctions above the predissociation limit.

UNCLASSIFIED

SECURITY CLASSIFICATION OF THIS PAGE(When Data Entered)

TABLE OF CONTENTS

	Page
LIST OF ILLUSTRATIONS	5
LIST OF TABLES	7
I. INTRODUCTION	9
II. EXPERIMENTAL DETAILS	11
III. DATA ANALYSIS AND RESULTS	17
IV. DISCUSSION	24
A. Absolute $q_{V'V''}$ for the B-X System	24
B. A Graphical Representation of the $q_{V'V''}$	24
C. Overlap with $\psi_{V'}$ above the Predissociation Limit	29
REFERENCES	33
APPENDIX A	35
APPENDIX B	37
DISTRIBUTION LIST	39

LIST OF ILLUSTRATIONS

Figure	Page
1. Schematic illustration of the experiment. The laser is tuned to a specific rotational line (rotational levels are not shown on the diagram) of the (9,1) band, exciting $v' = 9$. Emission is observed to many v'' levels, a few of which are indicated	12
2. Experimental arrangement. The narrow-band, tunable, frequency doubled dye laser irradiates the S ₂ , whose fluorescence is measured by a scanning monochromator (I) and monitored by another (II) at fixed wavelength. A boxcar integrator, triggered by the laser pulse, yields the ratio of the two outputs, which is integrated as well as recorded directly	13
3. Excitation scans of the (6,0) band. The laser wavelength is scanned while the output from monochromator II is measured. (Top) Laser bandwidth 12 cm ⁻¹ (Bottom). A small region of the scan shown on top, with the laser bandwidth here 0.3 cm ⁻¹	15
4. Scans of the fluorescence obtained exciting the $v' = 6$, $N' = 36$, $J' = 37$ level of B ³ Σ _u ⁻ . (a) Scan of the rotational structure in the (6,1) term. The R ₁ - P ₁ splitting is 3.85Å. A P _{R13} branch is also present but overlapped by the P ₁ line. (b) Scan of the entire fluorescence progression emitted by $v' = 6$. The asterisk marks the exciting band, (6,0). Terms are visible here out to $v'' = 26$. Each term consists of the same rotational structure shown in (a) . . .	16
5. (Left) Potential curves and several wavefunctions for the B and X states of S ₂ . (Right) Schematic replacement of the ground state wavefunctions by a gate attached at the right hand turning point. Increasing v'' in effect scans the gate to larger internuclear distance, tracing out $ \psi_{v'} ^2$ (see text)	26
6. A plot of the $q_{v'v''}$ vs. $r_R(v'')$; see text. The zero for each $q_{v'v''}$ is placed at the corresponding energy level for that v' . The curve is the B-state RKR potential, independently plotted	28
7. A plot of $q_{v'v''}$ vs. $r_L(v')$ as in Fig. 6; see text. The curve is an independently plotted X-state RKR potential . . .	31

LIST OF TABLES

Table	Page
1. FRANCK-CONDON FACTORS AND UNCERTAINTIES FOR $v' = 2$ EXCITED LEVEL IS F ₃ (46)	19
2. FRANCK-CONDON FACTORS AND UNCERTAINTIES FOR $v' = 6$ EXCITED LEVEL IS F ₁ (34)	20
3. FRANCK-CONDON FACTORS AND UNCERTAINTIES FOR $v' = 7$ EXCITED LEVEL IS F ₃ (30)	21
4. FRANCK-CONDON FACTORS AND UNCERTAINTIES FOR $v' = 8$ EXCITED LEVEL IS N' = 28	22
5. FRANCK-CONDON FACTORS AND UNCERTAINTIES FOR $v' = 9$ EXCITED LEVEL IS F ₁ (36)	23
6. FRANCK-CONDON FACTORS FOR THE B-X SYSTEM. ENTRIES ARE $1000 \times q_{v'v''}$, EXCEPT FOR THE LAST COLUMN, WHICH IS THE FRACTIONAL OVERLAP WITH THE CONTINUUM FOR THE v'' LEVEL	25

I. INTRODUCTION

A simple product form can often be written to express the relationship between the intensity of an emission line in an electronic transition of a diatomic molecule, and the population of the emitting level:

$$I_{v'J'}^{v''J''} = [64\pi^4 \nu^4 / 3c^2] [S_{J'J''} / (2J' + 1)] \bar{R}_e^2 q_{v'v''} N_{v'J'} \quad (1)$$

This represents the total energy (erg) emitted each second (into all 4π sterad) from 1 cm^3 of gas containing $N_{v'J'}$ excited state molecules in the level in question. ν is the frequency (Hz) of the transition, which occurs between the upper (single prime) and lower (double prime) vibrational (v) and rotational (J) states. The electronic transition moment \bar{R}_e is here assumed constant for all transitions, an assumption valid¹ for the B-X system of S_2 studied in this work. The contributions due to the nuclear motion, viz., the rotational line strength $S_{J'J''}$ and the vibrational overlap factor (Franck-Condon factor) $q_{v'v''}$, are likewise considered in Eq. (1) to be fully separable. (Small, calculable corrections to the ν -dependence of $S_{J'J''}$ and the J -dependence of $q_{v'v''}$ have been discussed.)¹

There is a variety of experiments in which intensity data are used, together with Eq. (1), to extract populations of individual levels in both ground and excited states. Such applications require reliable values of $S_{J'J''}$ and $q_{v'v''}$ for the electronic system under study. For the $B^3\Sigma_u^- - X^3\Sigma_g^-$ system of S_2 , there have been several such investigations recently. These include data on energy transfer within the B-state following selective excitation,² and the analysis of chemiluminescence produced in afterglows^{3,4} or following the alkaline earth rearrangement

¹K. A. Meyer, "Some Radiative Properties of the $B^3\Sigma_u^-$ State of Diatomic Sulfur", Ph. D. Thesis, University of Wisconsin, 1976; K. A. Meyer and D. R. Crosley, "Intensity Studies on S_2 Selectively Excited by Hg Line Radiation", to be published.

²T. A. Caughey, "Collisional Energy Transfer in B State Diatomic Sulfur", Ph. D. Thesis, University of Wisconsin, 1977; T. A. Caughey and D. R. Crosley, "Relaxation Within the $B^3\Sigma_u^-$ State of S_2 ", *J. Chem. Phys.*, **69**, 3379 (1978).

³D. Kley and H. P. Broida, "Chemiluminescence and Photoluminescence of S_2 , SO and SO_2 in SF_6 Afterglows", *J. Photochem.*, **6**, 241-252 (1976/77).

⁴G. Lakshminarayana and C. G. Mahajan, "Spectroscopic Studies of the Sulfur Afterglow", *J. Quant. Spectrosc. Radiat. Transfer*, **16**, 549-552 (1976).

reaction $M + S_2Cl_2$.⁵ Another application lies in the choice of broad-band filtering for flame photometric analysis of sulfur in the presence of interferences.⁶

As a probe of ground state populations, laser induced fluorescence such as reported here is a most attractive diagnostic tool; at least one other current study⁷ has used this technique as a combustion diagnostic for S_2 . In addition, photoluminescence from a filtered continuum³ can also provide ground state data. Finally, these data can be used for further development of the recent optically pumped S_2 laser,⁸ which has a broad range of near continuous tunability through the ultra-violet and visible; the widespread occurrence of B-X emission in discharges and chemical reactions offers the possibility of an S_2 chemical laser.

In nearly all cases of diatomic electronic transitions, including the B-X system of S_2 , sufficiently accurate values of $S_j'j''$ may be obtained by calculation, using measured spectroscopic constants. The Franck-Condon factors can also be theoretically computed to the required accuracy in many cases, using model potentials, most often of RKR form. In the case of the B-X transition, however, such calculations of $q_{v'v''}$ are not reliable, as is illustrated⁹ by the disagreement between experimental and calculated values of $q_{3,v''}$ and $q_{4,v''}$ for $v'' = 0$ through 10. While the calculated Franck-Condon factors exhibit the same qualitative trends as those seen in the measured values, the quantitative disagreement precludes the use of the theoretical quantities for analysis purposes, so that experimental values are necessary.

⁵F. Engelke and R. N. Zare, "Crossed-Beam Chemiluminescence: The Alkaline Earth Rearrangement Reaction $M + S_2Cl_2 \rightarrow S_2^* + MCl_2$ ", *Chem. Phys.*, **19**, 327-340 (1977).

⁶S. S. Brody and J. E. Chaney, "The Application of a Specific Detector for Phosphorous and for Sulfur Compounds - Sensitive to Nanogram Quantities", *J. Gas Chromatog.*, **4**, 42-46 (1966); P. J. Maroulis and A. R. Bandy, "Estimate of the Contribution of Biologically Produced Dimethyl Sulfur to the Global Sulfur Cycle", *Science*, **196**, 647 (1977).

⁷C. H. Moeller, II, K. Schofield, M. Steinberg, and H. P. Broida, "Sulfur Chemistry in Flames", *Seventeenth Symposium (International) on Combustion*, Leeds, England, August 1978.

⁸S. R. Leone and K. G. Kosnik, "A Tunable Visible Ultraviolet Laser on S_2 ($B^3\Sigma_u^- - X^3\Sigma_g^-$)", *Appl. Phys. Lett.*, **30**, 346-348 (1977).

⁹K. A. Meyer and D. R. Crosley, "Franck-Condon Factors From Selectively Excited Resonance Fluorescence in the B-X System of S_2 ", *J. Chem. Phys.*, **59**, 3153-3161 (1973).

Although the B-X system in discharge emission is too heavily congested to permit reliable intensity measurements over but a small range of bands, it is an ideal candidate for study using the technique of selective excitation of resonance fluorescence. The method is schematically illustrated in Figure 1. A laser is tuned to some specific absorption line of the (9,1) band, exciting the S₂ to a particular triplet component of a particular rotational level in $v' = 9$ (the rotational and triplet structure is not explicitly shown in Figure 1). From here the S₂ radiates to all of the v'' levels for which the $q_{v'v''}$ are non-negligible; several of these are indicated in the figure. The experiment consists of the measurement of the relative intensities of these transitions; because all the fluorescent terms are monitored, absolute values of $q_{v'v''}$ may be extracted from the data.

Earlier work by Meyer^{1,9} utilized atomic line selective excitation of individual $v'J'$ levels of the $B^3\Sigma_u^-$ state, furnishing the Franck-Condon factors for $v' = 0, 1, 3, 4$, and 5. In the current study, a frequency doubled, tunable dye laser has served as the excitation source, enabling measurements to be made on $v' = 2$ and 6 through 9. The combination of these results forms the full set of $q_{v'v''}$ for all the bound-bound vibrational bands of the B-X system of the 32-32 isotope.

II. EXPERIMENTAL DETAILS

The apparatus used in the experiment is illustrated schematically in Figure 2. The sulfur is maintained in an evacuable all-quartz cell; the pressure is held at ~ 100 mtorr by a sidearm reservoir at $\sim 110^\circ\text{C}$, and the body cell is kept at $\sim 600^\circ\text{C}$ to ensure a high concentration ($> 98\%$) of the S₂ species. The exciting photons are provided by a flashlamp pumped dye laser which is frequency doubled (Chromatix CMX4), and into which an intracavity etalon may be inserted.

Several parameters are monitored during an experiment in order to prevent errors caused by drift in either the laser intensity or frequency. The essential results of the experiment are provided by a scanning 0.35m monochromator (#I), outfitted with an EMI 9558Q photomultiplier (PMT) and usually operated with 75 μ slits. After preamplification, and subsequent attenuation if necessary, the PMT output is fed to channel A of a dual-input boxcar integrator. A second monochromator, #II, having an EMI 6255 PMT detector, is operated with wide slits (2 mm) and at a fixed wavelength. This wavelength corresponds to that of one of the more intense terms of the fluorescent series emitted by the particular v' excited by the laser. After preamplification, this forms the input to channel B. In addition, a small portion of the ultraviolet light is split off prior to entering the sulfur cell, and detected by a third PMT whose average current is measured. The input to channels A or B, and the corresponding boxcar gages, are observed on an oscilloscope. Recorder traces are made of the boxcar output of channel A \div channel B v. the wavelength of monochromator I, and the integral of this quantity over wavelength for each

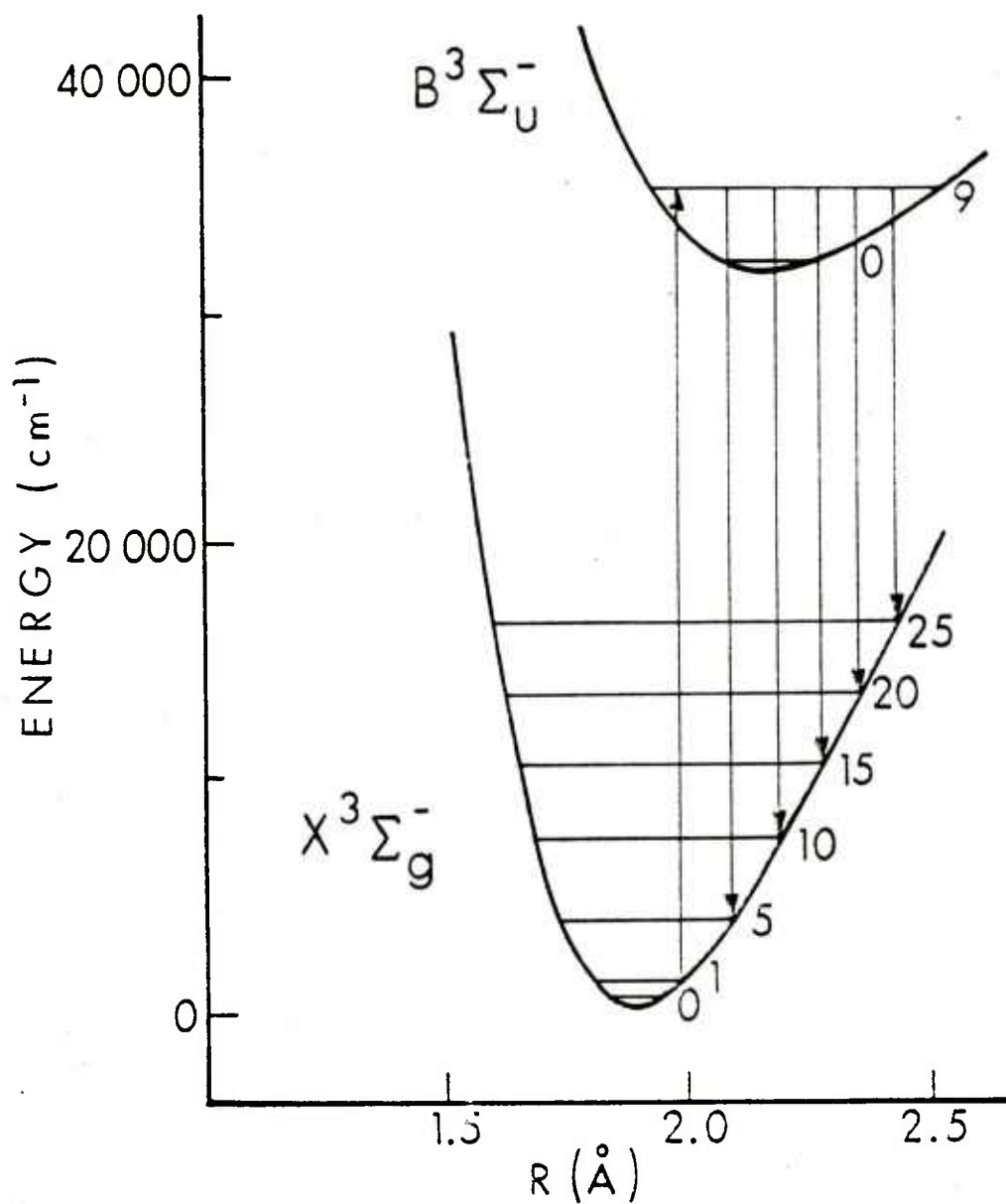


Figure 1. Schematic illustration of the experiment. The laser is tuned to a specific rotational line (rotational levels are not shown on the diagram) of the (9,1) band, exciting $v' = 9$. Emission is observed to many v'' levels, a few of which are indicated.

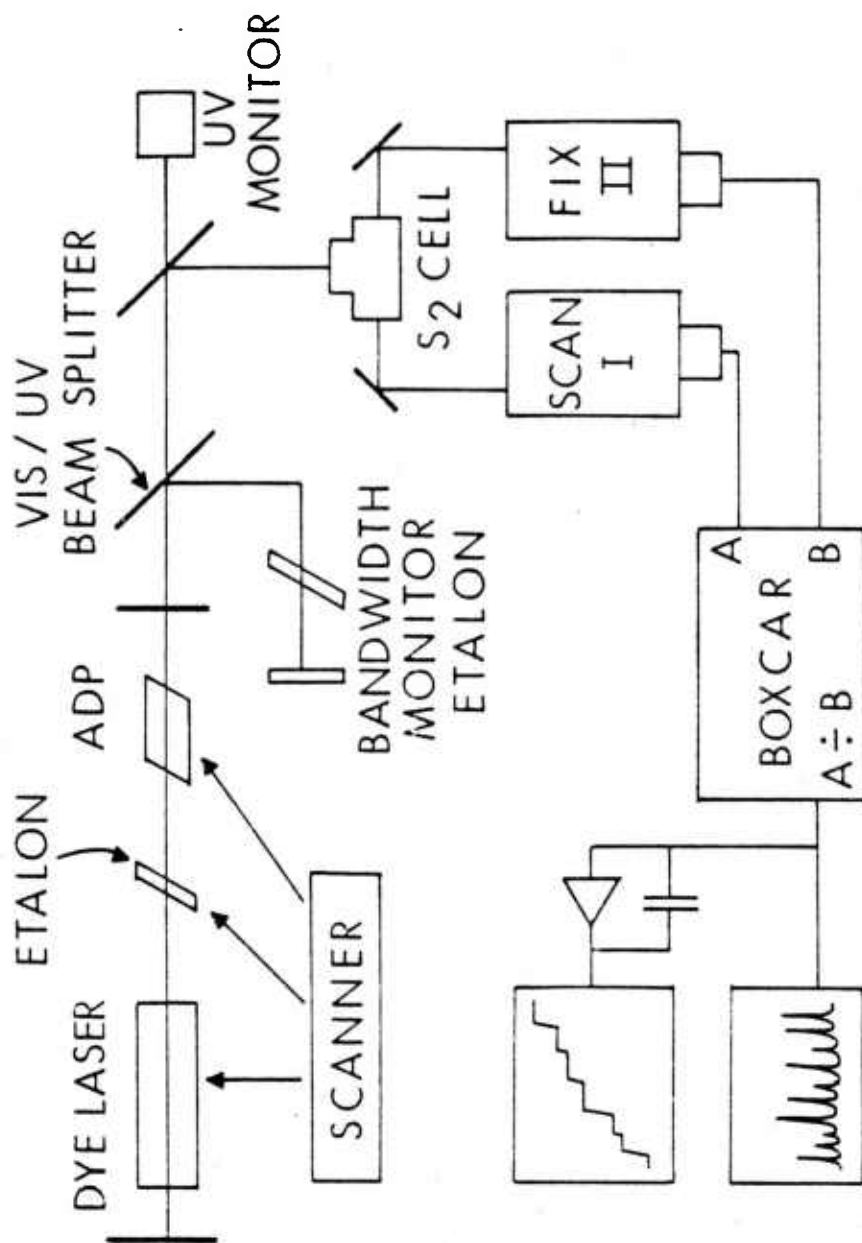


Figure 2. Experimental arrangement. The narrow-band, tunable, frequency doubled dye laser irradiates the S₂, whose fluorescence is measured by a scanning monochromator (I) and monitored by another (II) at fixed wavelength. A boxcar integrator, triggered by the laser pulse, yields the ratio of the two outputs, which is integrated as well as recorded directly.

band which forms the raw experimental data). Also, we monitor, and sometimes record, the output of channel B, providing a measure of the laser amplitude and frequency drift, and the ultraviolet-detecting PMT, which yields a measure of the laser power. In addition, the small amount of visible light emitted by the laser passes through a small etalon; the resulting fringe pattern on a screen is checked visually to ensure that the proper line narrowing by the intracavity etalon is maintained.

A 20 cm long fiber optic rod collects light from the flashlamp and delivers it to an enclosed photodiode mounted above a fast amplifier. The photodiode output forms the trigger pulse for the boxcar and scope. An earlier mode of triggering using a synchronization pulse keyed to the laser spark gap circuitry proved unreliable due to jitter in the flashlamp firing time, whereas the photodiode trigger was quite stable.

The bandwidth of the laser, in the etalon-narrowed configuration used for the runs, is $\sim 0.3 \text{ cm}^{-1}$ in the ultraviolet. Individual rotational absorption lines were often congested even on this scale, and some effort was necessary in order to find a line in each absorption band which was free of overlap. The laser was first scanned in the unnarrowed mode ($\sim 10 \text{ cm}^{-1}$ bandwidth) and the fluorescence monitored, as a function of laser wavelength, by monochromator, II. This produces an excitation spectrum such as that shown in Figure 3 for a scan of the (6,0) band. Narrowing the laser line and scanning a smaller region produces the more highly resolved excitation spectrum also shown in Figure 3, though this is still not fully free from overlapped excitation lines. After choosing a suitable candidate for excitation, the rotationally resolved fluorescence spectrum for a given term or terms is scanned with monochromator I. This produces a characteristic two or three-line pattern whose spectral purity is further ascertained by slight detuning of the laser, and rescanning to check for overlap.

In Figure 4 is shown an exemplary recorder tracing of the fluorescence progression obtained by scanning monochromator I while exciting the $N' = 36$, $J' = 37$ level of $v' = 6$. Each term consists of the apparent three-line pattern shown expanded for $v'' = 1$. The seven-lobe undulatory pattern in the scan admits of a simple interpretation discussed more fully below.

The response of the monochromator-PMT combination as a function of wavelength was measured using a GE DXW tungsten halide lamp with an NBS-traceable calibration curve.

It is necessary to ascertain that reabsorption of the emission by ground state S_2 , between the emitting region and the cell exit window, does not affect the measured results for the low v'' terms. Intensities were measured for at least three reservoir temperatures encompassing that used for the actual runs, and an extrapolation was made to zero pressure. See Appendix I for further details.

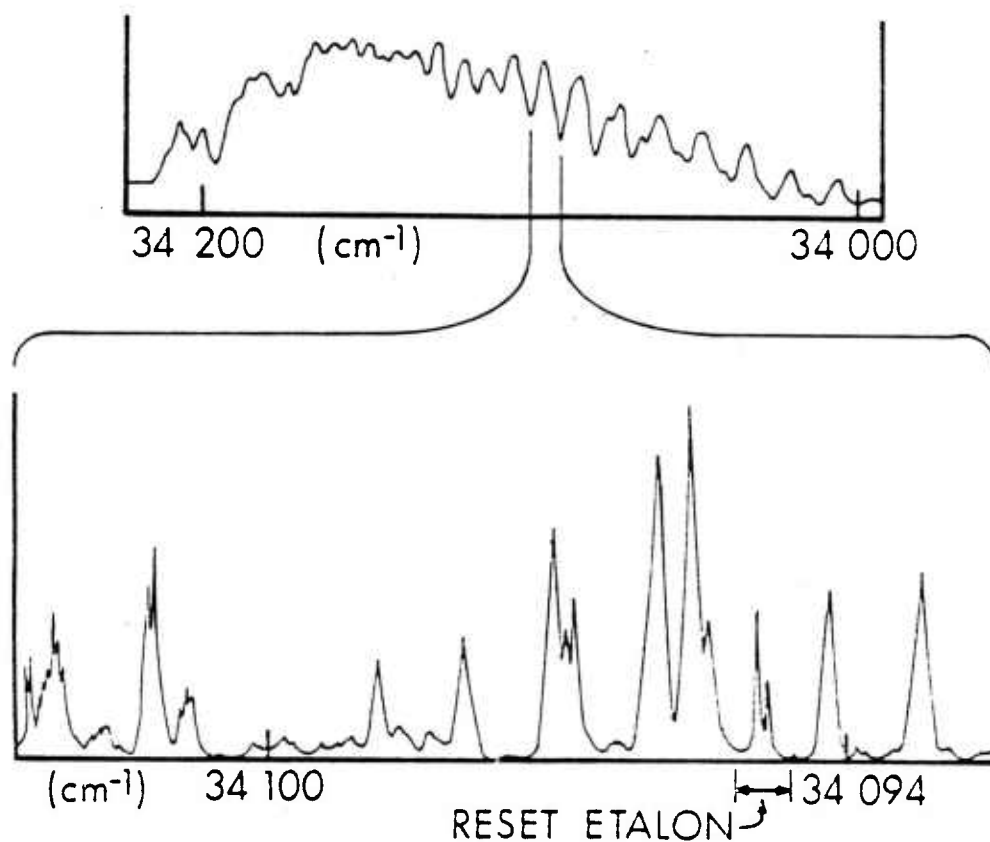


Figure 3. Excitation scans of the (6,0) band. The laser wavelength is scanned while the output from monochromator II is measured. (Top) Laser bandwidth 12 cm^{-1} (Bottom). A small region of the scan shown on top, with the laser bandwidth here 0.3 cm^{-1} .

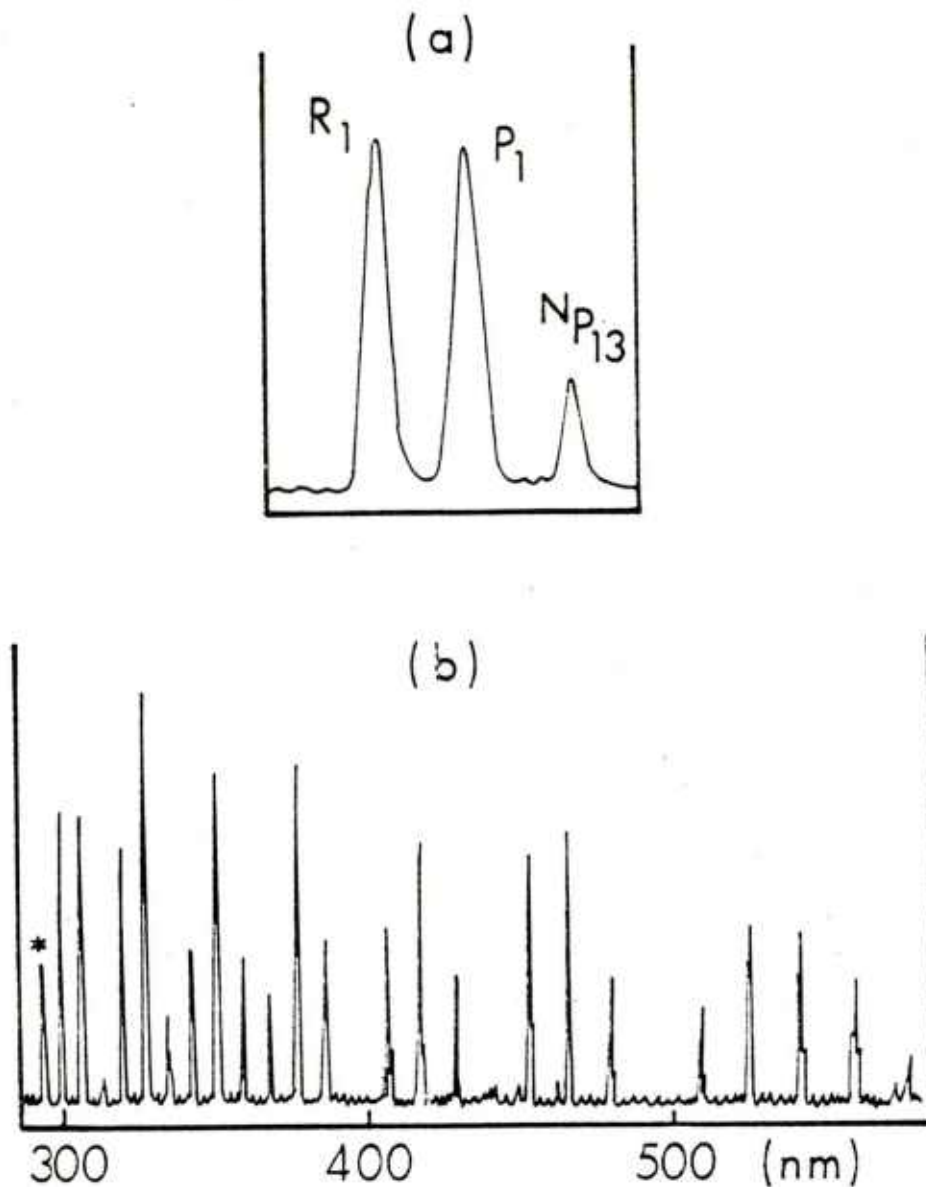


Figure 4. Scans of the fluorescence obtained exciting the $v' = 6$, $N' = 36$, $J' = 37$ level of $B^3\Sigma_u^-$. (a) Scan of the rotational structure in the (6,1) term. The $R_1 - P_1$ splitting is 3.85Å. A P_{13} branch is also present but overlapped by the P_1 line. (b) Scan of the entire fluorescence progression emitted by $v' = 6$. The asterisk marks the exciting band, (6,0). Terms are visible here out to $v'' = 26$. Each term consists of the same rotational structure shown in (a).

III. DATA ANALYSIS AND RESULTS

The measured intensity for a particular v'' term, $F_{v'v''}$ is obtained from the recorder trace representing the integral, over the full wavelength range of that term, of the A B boxcar input. While this normalization provides adequate correction for small drifts in laser power, the doubling crystals must occasionally be peaked up during the scan of a single progression. When such drift is present, a term of low v'' having high measured intensity is rescanned to provide correct ratios.

For the fluorescent term corresponding to the excitation band, there is some laser scatter present at the wavelength of the exciting rotational branch. The intensity for this particular term is then obtained from the ratio of the peak heights of the non-overlapped rotational branch in that term, and the corresponding rotational branch of a neighboring intense term.*

These measured intensities are corrected for the detector response $R(v)$ and divided by the v^4 factor.** This yields a series of measured quantities strictly proportional to $\sum J'' \overline{R_e^2} S_{J'J''} q_{v'v''}$. We assume that the electronic transition moment is independent of internuclear distance, so that $\overline{R_e^2}$ is the same for all (v', J', v'', J'') . This constancy is borne out by the lack of any discernible overall smooth trends in the $q_{v'v''}$ measured here or previously;^{1,9} a more complete discussion of this point may be found elsewhere.¹ Since we integrate over all the rotational branches of the fluorescent emission, and since $\sum J'' S_{J'J''} = 2J' + 1$, no corrections for the vibrational dependence¹⁰ of $S_{J'J''}$ need be made. Thus, the $F_{v'v''}/v^4 R(v)$ form a set of values, each proportional to the Franck-Condon factor $q_{v'v''}$ for that term.

Now the sum, over all v'' , of the $q_{v'v''}$ for a particular v' , is unity:

$$\sum_{v''} q_{v'v''} = 1 \quad . \quad (2)$$

* This also alleviates concerns about contributions due to stimulated emission, which is present in the rotational branch overlapped by the laser, at the spectral power densities used.

** The PMT actually measure photons sec^{-1} , not erg sec^{-1} , but the calibration using the standard lamp is done so as to obtain an effective response in the latter units.

¹⁰ Such a correlation should be applied to the intensities of the rotationally resolved branches used to determine the intensity of the excitation term; however, this is a negligible amount. See K. A. Meyer and D. R. Crosley, "Rotational Satellite Intensities and Triplet Splitting in the $B^3\Sigma_u^-$ State of S_2 ", *Can. J. Phys.*, 51, 2119-2124 (1973).

The rationale for this relationship is perhaps most readily evident by an expansion of the upper state vibrational wavefunction $\psi_{V'}$ in terms of the complete set of ground state vibration wavefunctions $\psi_{V''}$:

$$\psi_{V'} = \sum_{V''} a_{V'V''} \psi_{V''}$$

But

$$|a_{V'V''}|^2 = \left| \int \psi_{V'}(r) \psi_{V''}(r) dr \right|^2 \equiv q_{V'V''} \quad (3)$$

(where r is the internuclear distance), and the orthonormality of the $a_{V'V''}$ directly yields Eq. (2). It is necessary in this context to note that the continuum vibrational wavefunctions of the X-state lie above the bound vibrational wavefunctions of the B-state, so that the sum is effectively over the bound wavefunctions only.

Consequently, by Eq. (2), the normalization of our measured intensities to unit sum directly yields the absolute Franck-Condon factor for each term. This is possible since the cleanliness of the emission afforded by the selective excitation process permits us to measure all of the terms in the fluorescence progression. The values obtained are collected in Tables 1 through 5.

The uncertainty in the individual measured intensity of each term, $\delta F_{V'V''}$, has been estimated from the chart recorder output. The resulting error bars in the $q_{V'V''}$ are of two kinds, both of which are listed in Tables 1 through 5. The first, designated $\delta q_{V'V''}$, is directly proportional to the measured uncertainty $\delta q_{V'V''} = q_{V'V''} \delta F_{V'V''} / F_{V'V''}$. This is the pertinent uncertainty to be used when comparing the ratio of any of the measured Franck-Condon factors, e.g., in a determination of the temperature or a measurement of product distributions in chemiluminescence.

The uncertainties $\delta q_{V'V''}$ also lead to a total uncertainty in the sum used for the normalization. Consequently, the uncertainty in the absolute value of each $q_{V'V''}$ contains a contribution from this source as well as from the $\delta q_{V'V''}$. These uncertainties in the absolute Franck-Condon factors, termed $\Delta q_{V'V''}$, are those necessary for such purposes as absolute absorption strength calculations, and laser design considerations. The $\Delta q_{V'V''}$ are calculated as the square root of the sum of the squares of $\delta q_{V'V''}$ and the normalization uncertainty.

It should be stressed that our values of $q_{V'V''}$ are of course only as accurate as the calibration of the spectrometer and PMT using the standard lamp. Since we require only the relative output of the lamp as a function of wavelength, an uncertainty of the order of only 1-2%

TABLE I. FRANCK-CONDON FACTORS AND UNCERTAINTIES FOR $v' = 2$
EXCITED LEVEL IS F_3 (46)

v''	$10^3 q$	$10^3 \delta q$	$10^3 \Delta q$
0	1.3	0.2	0.2
1	11.7	0.4	0.7
2	40.3	3.8	4.4
3	112.7	2.9	6.7
4	116.1	5.0	8.0
5	77.0	2.0	4.6
6	20.0	1.2	1.6
7	4.5	0.5	0.6
8	40.5	1.8	2.8
9	72.6	3.1	5.0
10	60.3	1.8	3.7
11	16.3	1.5	1.7
12	1.6	0.6	0.6
13	21.5	1.5	1.9
14	65.2	3.7	5.1
15	72.3	3.4	5.2
16	101.6	3.3	6.4
17	76.4	2.6	4.9
18	45.6	2.1	3.2
19	21.5	1.9	2.2
20	14.5	1.4	1.6
21	6.5	2.6	2.6
22	<2.0	2.0	---

TABLE 2. FRANCK-CONDON FACTORS AND UNCERTAINTIES
FOR $v' = 6$ EXCITED LEVEL IS $F_1(34)$

v''	$10^3 q$	$10^3 \delta q$	$10^3 \Delta q$
0	26.6	5.4	6.2
1	76.6	2.4	8.8
2	53.5	2.2	6.3
3	3.4	0.8	0.9
4	32.1	3.2	4.8
5	58.3	4.1	7.7
6	5.5	1.8	1.9
7	21.2	2.5	3.4
8	50.8	2.1	6.0
9	13.1	1.3	2.0
10	7.3	1.8	2.0
11	48.8	2.0	5.8
12	27.1	1.0	3.2
13	2.0	1.0	1.0
14	29.0	1.1	3.4
15	47.1	1.6	5.5
16	13.0	1.8	2.3
17	<1.8	1.8	---
18	66.8	4.1	8.5
19	77.5	5.3	10.1
20	21.3	8.9	9.2
21	9.7	4.9	5.0
22	29.4	4.7	5.7
23	75.5	7.7	11.4
24	69.2	4.6	9.0
25	69.9	12.5	14.7
26	37.7	9.4	10.3
27	27.4	13.7	14.0
28	<10.0	10.0	---

TABLE 3. FRANCK-CONDON FACTORS AND UNCERTAINTIES
FOR $v' = 7$ EXCITED LEVEL IS F_3 (30)

v''	$10^3 q$	$10^3 \delta q$	$10^3 \Delta q$
0	46.5	1.4	5.4
1	79.6	7.7	11.7
2	40.6	1.8	4.9
3	8.2	2.1	2.3
4	62.9	4.5	8.3
5	24.9	4.2	5.0
6	9.0	2.8	3.0
7	15.0	0.6	1.8
8	20.5	2.5	3.4
9	7.8	2.6	2.7
10	44.3	2.7	5.6
11	22.3	1.1	2.7
12	<1.9	1.9	---
13	38.1	2.5	4.9
14	28.6	2.9	4.3
15	<2.0	2.0	---
16	28.7	3.0	4.4
17	38.8	3.3	5.4
18	22.0	2.8	3.7
19	<1.9	1.9	---
20	50.2	5.0	7.5
21	68.6	4.9	9.1
22	27.1	5.4	6.2
23	<2.0	2.0	---
24	19.8	5.0	5.5
25	16.6	9.2	11.5
26	86.0	7.7	12.3
27	64.2	6.4	9.6
28	54.6	9.1	10.9
29	30.1	10.0	10.5
30	<2.0	2.0	---

TABLE 4. FRANCK-CONDON FACTORS AND UNCERTAINTIES FOR
 $v' = 8$ EXCITED LEVEL IS $N' = 28$

v''	$10^3 q$	$10^3 \delta q$	$10^3 \Delta q$
0	43.0	4.6	5.7
1	71.9	2.9	6.3
2	4.4	0.6	0.7
3	37.9	3.0	4.2
4	50.7	3.2	5.1
5	<0.6	0.6	---
6	43.5	3.1	4.6
7	38.0	3.1	4.3
8	0.9	0.4	0.4
9	44.1	2.5	4.2
10	24.7	1.3	2.3
11	3.2	0.1	0.3
12	45.8	2.3	4.2
13	23.7	1.4	2.3
14	1.8	0.1	0.2
15	39.1	1.8	3.5
16	28.2	1.0	2.4
17	<0.2	0.2	---
18	29.0	1.3	2.6
19	46.7	1.7	4.0
20	8.6	0.4	0.8
21	6.3	0.6	0.8
22	42.4	2.1	3.9
23	45.6	2.4	5.0
24	12.5	1.2	1.5
25	2.3	1.2	1.2
26	31.7	1.0	2.7
27	65.9	3.0	5.9
28	76.9	7.6	9.7
29	74.1	4.9	7.6
30	36.8	8.6	9.1
31	20.0	10.0	10.1
32	<2.0	2.0	---

TABLE 5. FRANCK-CONDON FACTORS AND UNCERTAINTIES FOR
 $v' = 9$ EXCITED LEVEL IS F_1 (36)

v''	$10^3 q$	$10^3 \delta q$	$10^3 \Delta q$
0	82.5	11.7	14.6
1	70.2	3.5	8.2
2	0.6	0.2	0.2
3	57.8	2.9	6.7
4	23.0	1.1	2.7
5	14.7	0.8	1.7
6	53.4	2.7	6.2
7	2.0	0.4	0.5
8	35.1	1.8	4.1
9	40.0	2.0	4.7
10	0.3	0.1	0.1
11	39.1	2.0	4.6
12	22.9	1.2	2.7
13	3.8	0.2	0.4
14	43.2	2.1	5.0
15	18.5	1.2	2.3
16	3.9	0.2	0.5
17	38.3	1.9	4.4
18	25.9	1.8	3.3
19	0.6	0.4	0.4
20	31.9	3.7	5.0
21	39.9	2.0	4.6
22	5.1	0.7	0.9
23	11.2	1.2	1.7
24	41.6	3.3	5.5
25	35.9	2.4	4.5
26	6.2	1.9	2.0
27	2.0	1.0	1.0
28	31.6	5.5	6.4
29	64.7	5.5	8.7
30	91.2	10.0	13.8
31	50.5	6.1	8.1
32	12.2	6.1	6.2
33	<6.0	6.0	---

in the absolute $q_{v'v''}$ is estimated¹ as arising from the calibration. This is not included in the numerical values for $\Delta q_{v'v''}$ given in the tables.

For each excitation, the values of J' for the level excited are determined by a measurement of the splitting¹¹ between the main R-P doublet (See Figure 4a) for several intense terms in the progression. Appendix II contains details concerning the analysis; the result for each excitation is listed in the tables of $q_{v'v''}$. The Franck-Condon factors in S_2 are observed¹ to vary somewhat with J' . However, the amount of the variation¹ is such that the reported values of $q_{v'v''}$, measured here for J' in the vicinity of 30, are quantitatively correct* for J' between 1 and approximately 50. This includes the important band head region, and the J' corresponding to the peak of the rotational distribution for temperatures of 2000° or less.

IV. DISCUSSION

A. Absolute $q_{v'v''}$ for the B-X System

Together with the measurements made by Meyer,^{1,9} these results complete the set of Franck-Condon factors for the B-X system of $^{32}S_2$. All of the values are collected in Table 6, where the entries are given (for convenience) in the form $1000q_{v'v''}$.

B. A Graphical Representation of the $q_{v'v''}$

A simple undulatory pattern, like that exhibited in Figure 4b for the fluorescence progression emitted by $v' = 6$, is observed for each v' . In particular, the locus of the peaks of the intensities forms a pattern always having $(v' + 1)$ lobes. This result is amenable to a simple explanation⁹ and a graphical representation which are described in the following.

Referring to Figure 1, it can be seen that the B-state vibrational wavefunctions have significant amplitude only over a range of internuclear distance where the ground state potential is attractive. This means that the primary contribution of $\psi_{v''}$ to $q_{v'v''}$ will come from the region nearer the right hand turning point, $r_R(v'')$, for that v'' .

In the left hand part of Figure 5, the $v' = 9$ and several v'' wavefunctions are drawn. Consider the overlap of $v' = 9$ with $v'' = 20$. The more rapid oscillations in the center of the $v'' = 20$ wavefunction will

¹¹K. A. Meyer and D. R. Crosley, "Hanle Effect Lifetime Measurements on Selectively Excited Diatomic Sulfur", *J. Chem. Phys.*, 59, 1933-1941 (1973).

*I. e. within the quoted error bars.

TABLE 6. FRANCK-CONDON FACTORS FOR THE B-X SYSTEM. ENTRIES ARE
 $1000 \times q_{v'v''}$, EXCEPT FOR THE LAST COLUMN, WHICH IS THE
 FRACTIONAL OVERLAP WITH THE CONTINUUM FOR THE v'' LEVEL

v''	v'	0	1	2	3	4	5	6	7	8	9	f
0	<1	1	1	4	9	15	27	47	43	83		0.77
1	1	6	12	21	39	48	77	80	72	70		0.57
2	10	25	40	67	82	80	54	41	4	1		0.60
3	23	55	113	100	69	39	3	8	38	58		0.49
4	41	103	116	72	11	14	32	63	51	23		0.47
5	64	112	77	6	11	43	58	25	<1	15		0.59
6	105	98	20	17	61	57	6	9	44	53		0.53
7	136	70	5	67	54	9	21	15	38	2		0.58
8	152	<3	41	69	5	18	51	21	1	35		0.61
9	143	23	73	20	16	56	13	8	44	40		0.56
10	118	45	60	3	62	29	7	44	25	<1		0.61
11	82	82	16	48	46	<3	49	22	3	39		0.61
12	58	100	2	76	3	28	27	<2	46	23		0.64
13	38	93	22	54	15	6	2	38	24	4		0.70
14	16	80	65	6	56	20	29	29	2	43		0.65
15	7	65	72	7	54	<4	47	<2	39	19		0.69
16	2	29	102	38	21	31	13	29	28	4		0.70
17	<1	20	76	72	1	50	<2	39	<1	38		0.70
18		<10	46	87	27	41	67	22	29	26		0.66
19			22	72	74	11	78	<2	47	1		0.70
20			15	47	87	15	21	50	9	32		0.72
21			7	32	77	61	10	69	6	40		0.70
22			<2	11	62	76	29	27	42	5		0.75
23				3	34	66	76	<2	46	11		0.76
24				<2	17	60	69	20	13	42		0.78
25					7	42	70	17	2	36		0.83
26					<1	15	38	86	32	6		0.82
27						13	27	64	66	2		0.83
28						<16	<10	55	77	32		0.84
29								30	74	65		0.83
30								<2	37	91		0.87
31									20	51		0.93
32									<2	12		0.99
33										<6		----
Ref.		1	1	--	9	9	1	--	--	--	--	

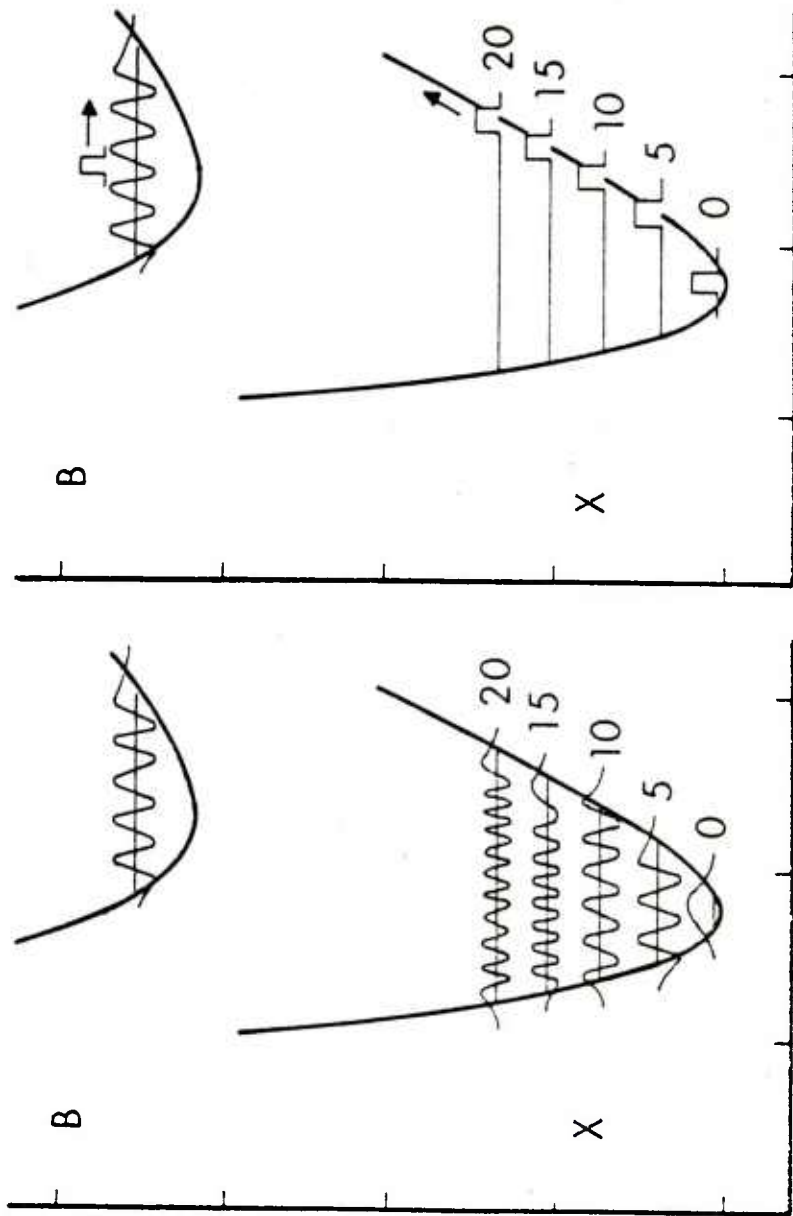


Figure 5. (Left) Potential curves and several wavefunctions for the B and X states of S_2 . (Right) Schematic replacement of the ground state wavefunctions by a gate attached at the right hand turning point. Increasing v in effect scans the gate to larger internuclear distance, tracing out $|\psi_v|^2$ (see text).

yield alternating positive and negative values when multiplied by the more slowly varying $\psi_{v'}$ at the same value of r (See Eq. (3)). Consequently, the contributions to the overlap integral from the middle region of internuclear distance will tend to cancel, and the integral will be dominated by contributions from the region near $r_R(v'')$ where $\psi_{v''} = 20$ has a more slowly varying amplitude.

This argument is extended graphically in the right hand portion of Figure 5, where the more rapidly oscillating part of the $\psi_{v''}$ (which give zero or small net overlap) is set to zero, and the lobe near $r_R(v'')$ replaced by a gate attached at the turning point. As the spectrometer scans the fluorescent progression, as in Figure 4b, the gate moves to higher v'' and hence, larger $r_R(v'')$ in effect scanning across $\psi_{v'}$ (See Figure 5). Considering the gate to be represented mathematically as a delta function, we have

$$q_{v',v''} = \left| \int \psi_{v'}(r) \delta(r - r_R(v'')) dr \right|^2 = \left| \psi_{v'}(r_R(v'')) \right|^2. \quad (4)$$

That is, the Franck-Condon factor $q_{v',v''}$ represents the square of the probability amplitude for the v' vibrational level at the value of internuclear distance given by $r_R(v'')$.

[Clearly, Eq. (4) represents an approximation needed for the purposes of discussion, rather than a quantitative relationship. However, model calculations for $v' = 4$ using Morse wavefunctions¹² have been carried out. These show that, while one must integrate inward from $r_R(v'')$ for 3 or 4 oscillations of $\psi_{v''}$ before the cancellation becomes appreciable, qualitatively correct calculated values of $q_{4,v''}$ are obtained by terminating the integral after the first lobe at $r_R(v'')$.]

This simple picture can be graphically represented in the following fashion. The right hand turning points $r_R(v'')$ are obtained from RKR calculations¹³ on the ground state. The $q_{v',v''}$ from Table 6 are then plotted, in stick diagram fashion, as a function of $r_R(v'')$. For each v' , the $q_{v',v''}$ are plotted with zero at the corresponding energy level (that is, in the way that wavefunctions are often plotted).

The results are displayed in Figure 6. Superimposed on the $q_{v',v''}$ pattern is the RKR curve for the B-state.¹³ It is to be emphasized

¹²G. D. Brabson, "Calculation of Morse Wave Function with Programmable Desktop Calculators", *J. Chem. Ed.*, 50, 397-399 (1973).

¹³G. D. Brabson and R. L. Volkmar, "Calculation of Potential Energy Curves for S_2 Perturbed by a Frozen Inert Gas Matrix Environment", *J. Chem. Phys.*, 58, 3209-3215 (1973).

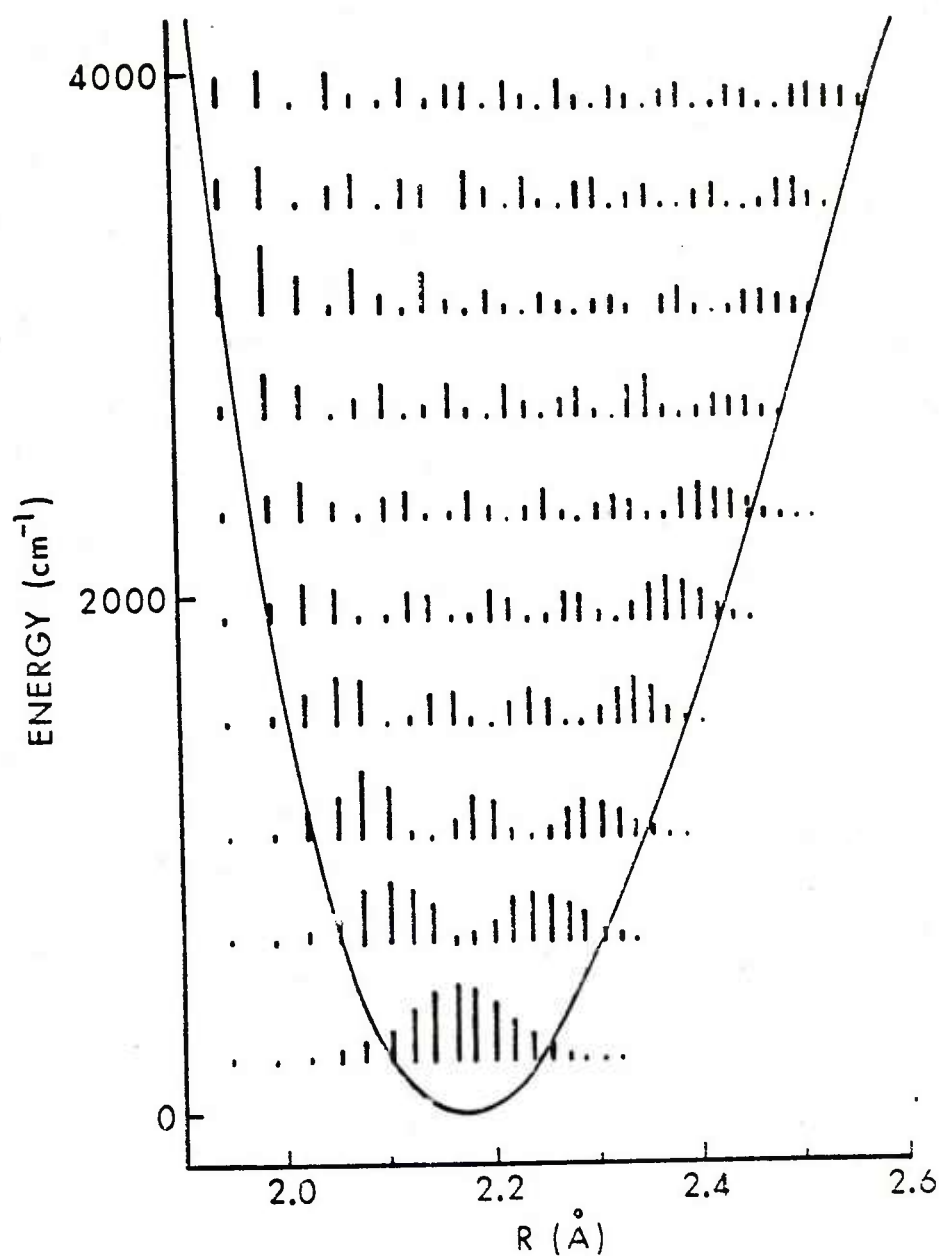


Figure 6. A plot of the $q_{v'v''}$ vs. $r_R(v'')$; see text. The zero for each $q_{v'v''}$ is placed at the corresponding energy level for that v' . The curve is the B-state RKR potential, independently plotted.

that the potential curve plot and the $q_{v'v''}$ plots shown in Figure 6 are entirely independent* of one another.

The assumptions involved in the use of Eq. (4) preclude attaching quantitative significance to Figure 6. Nonetheless, we find the representation exhibited there to be pleasing and instructive. The "wavefunctions" possess the proper number of lobes and span the expected range of internuclear distance with reasonable centering. It is tempting to point out, additionally, that the undulations in the center (where the kinetic energy is higher) have a shorter wavelength than those near the turning points, and that the plots show finite though small amplitude in the classically forbidden region outside the turning points. In any event, these results form a compelling reminder that molecular vibration is indeed described by a wavelike picture;¹⁴ in fact, the essence of this illustration is contained clearly in the raw data, such as that displayed in Figure 4b.

C. Overlap with $\psi_{v'}$ above the Predissociation Limit

The Franck-Condon factors, for a given $\psi_{v''}$, obey a sum rule like Eq. (2) when summed over v' . However, in this case the sum must also include those vibrational levels above the predissociation limit in $B^3\Sigma_u^-$, which sets in just below the rotationless level in $v' = 10$ (for the 32-32 isotope). One may write

$$\sum_{v'=0}^9 q_{v'v''} + f_{v''} = 1 \quad (5)$$

where $f_{v''}$ represents the fraction of the total overlap of $\psi_{v''}$ with those v' wavefunctions above this limit. The $f_{v''}$ may be easily evaluated by summing over the $q_{v'v''}$; the results are listed in Table 6.

A clear trend may be discerned in the $f_{v''}$. (A quantitative attempt at uncertainty assessment is unwarranted; small differences between any two $f_{v''}$ are likely not significant but the overall variation should be meaningful.) With the exception of $v'' = 0$, the overlap with the $\psi_{v'}$ above $v' = 9$ rises rather smoothly from a value near 50% for low v'' to a value above 90% for v'' in the vicinity of 30.

*The zero of energy must of course be defined.

¹⁴To quote the late E. U. Condon ["The Franck-Condon Principle and Related Topics", *Amer. J. Phys.*, **15**, 365-374 (1947)]: "The Franck-Condon patterns form real and forceful proof ... of the reality of de Broglie waves associated with the nuclear motions in the molecules". We thank Dr. R. N. Zare for drawing our attention to this delightful and instructive article.

The value of $f_{v''}$ for $v'' = 0$ is obviously outside the general trend. It is important to establish that this is a real difference, and not some systematic experimental error or artifact of the calculation procedure. To do so, we offer the following qualitative physical argument based on the same kind of approach used to arrive at the plot in Figure 6.

Again referring to Figure 1, we this time note that the $\psi_{v''}$, for low values of v'' , span a region of internuclear distance situated under the left-hand (repulsive) portion of the B-state potential. The same line of reasoning as before can now be used to consider that, for a given v'' , the set of $q_{v''}$ represents the values $|\psi_{v''}(r_L(v'))|^2$, the square of the probability amplitude at the left-hand turning point of the B-state potential. In this case, however, examination of Figure 1 suggests that the approximation should break down by the time $v'' \sim 10$.

In Figure 7 is presented a plot akin to that in Figure 6, for $0 < v'' < 10$. Brabson's calculations¹³ furnish the $r_L(v')$, as well as the X-state potential curve which is again independently* superimposed. The abrupt termination of the plots at $r_L(v' = 9) = 1.928\text{\AA}$ is of course due to the fact that the left-hand turning points less than this value belong to vibrational levels above the predissociation limit.

For the lowest values of v'' , one can discern the essential outlines of the right-hand portion of the "wavefunctions" showing reasonably spaced lobes of the proper number. On the other hand, the pattern becomes lost at the higher values of v'' plotted in Figure 7, as anticipated from the examination of the potentials.

Considering only a comparison of $\psi_{v''=0}$ with the $v'' = 1$ through 3 patterns, it can be seen that the former has a larger fraction of its amplitude in the region where $r < r_L(v' = 9)$. Consequently, it may be expected to have a significantly larger overlap with the predissociated levels $v' > 10$. Even though those v' levels are not bound, they too will have more slowly varying lobes near their (single) turning point at the repulsive wall. The $v'' = 0$ wavefunction exists in a region probably corresponding to that spanned by the rapidly rising B-state potential, yielding good overlap with these wavefunctions.

Herzberg and Mundie¹⁵ have taken absorption spectra of the $(v', 0)$ sequence up to $v' = 22$. The intensity in absorption jumps abruptly between $v' = 9$ and 10, corresponding to the onset of the predissociation. The relative intensities from $v' = 10$ through $v' = 22$ form a smooth pattern with a single maximum at $v' = 13$, strongly suggestive of the continuation, to the left, of the pattern for $v'' = 0$ in Figure 7. Their

*The zero of energy must of course be defined.

¹⁵G. Herzberg and L. G. Mundie, "On the Predissociation of Several Diatomic Molecules", *J. Chem. Phys.*, **8**, 263-273 (1940).

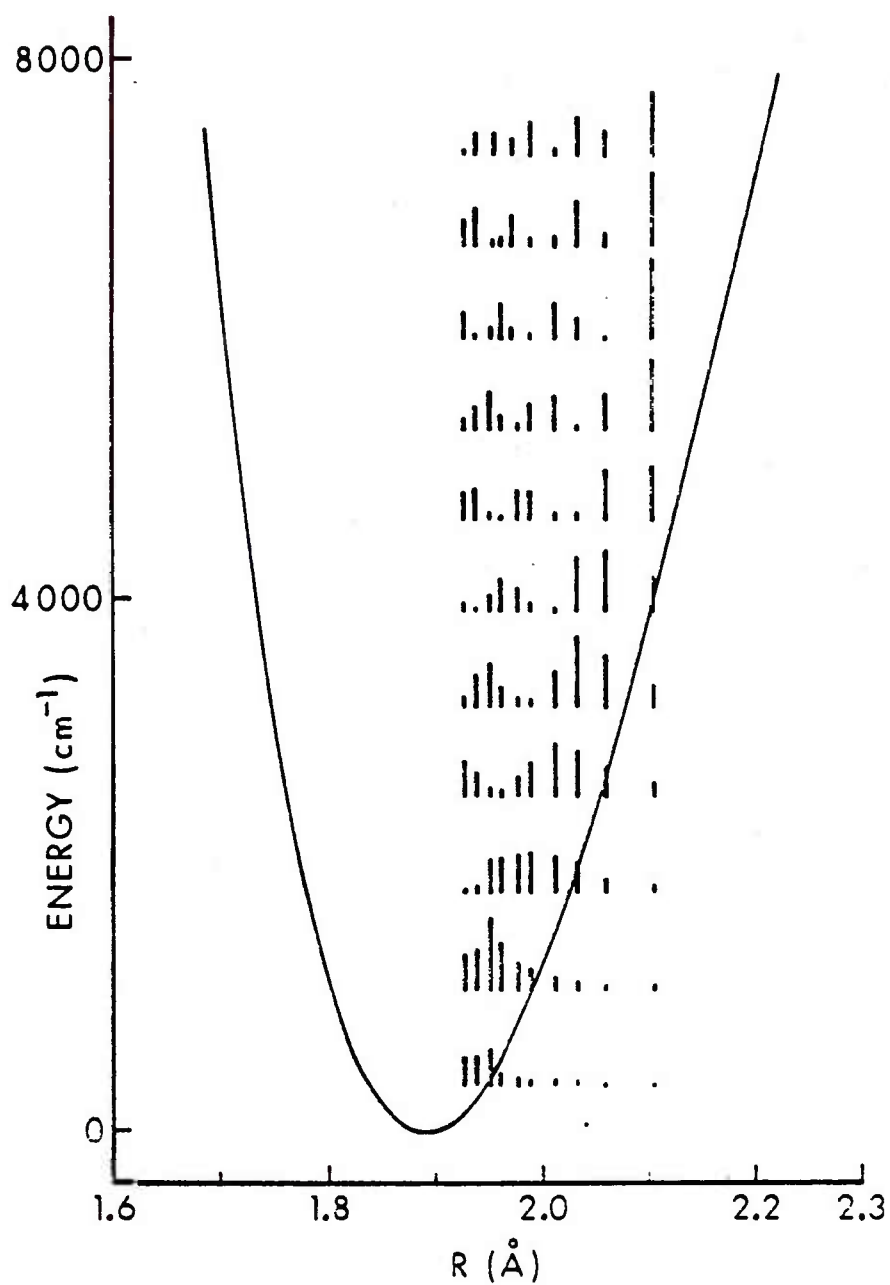


Figure 7. A plot of $q_{v'v''}$ vs. $r_L(v')$ as in Figure 6; see text. The curve is an independently plotted X-state RKR potential.

estimated intensities* indicate that 91% of the absorption strength out of $v'' = 0$ is to levels having $v' > 10$, while we have found that the overlap with these levels is only 75% of the total. This may indicate that the transition moment R_e is, on the average, about twice as large for the transitions to the predissociated levels as for the transitions to the bound ones. However, the likely variation in $R_e(r)$, on a state-by-state basis at high v' , renders this result useful only as a rough guide, and not as a quantitative characterization.

* Taken from the graph, Figure 2, of reference 15.

REFERENCES

1. K. A. Meyer, "Some Radiative Properties of the $B^3\Sigma_u^-$ State of Diatomic Sulfur", Ph. D. Thesis, University of Wisconsin, 1976; K. A. Meyer and D. R. Crosley, "Intensity Studies on S_2 Selectively Excited by Hg Line Radiation", to be published.
2. T. A. Caughey, "Collisional Energy Transfer in B State Diatomic Sulfur", Ph. D. Thesis, University of Wisconsin, 1977; T. A. Caughey and D. R. Crosley, "Relaxation Within the $B^3\Sigma_u^-$ State of S_2 ", J. Chem. Phys., 69, 3379 (1978).
3. D. Kley and H. P. Broida, "Chemiluminescence and Photoluminescence of S_2 , SO and SO_2 in SF_6 Afterglows", J. Photochem., 6, 241-252, (1976/77).
4. G. Lakshminarayana and C. G. Mahajan, "Spectroscopic Studies of the Sulfur Afterglow", J. Quant. Spectrosc. Radiat. Transfer, 16, 549-552 (1976).
5. F. Engelke and R. N. Zare, "Crossed-Beam Chemiluminescence: The Alkaline Earth Rearrangement Reaction $M + S_2Cl_2 \rightarrow S_2^* + MCl_2$ ", Chem. Phys., 19, 327-340 (1977).
6. S. S. Brody and J. E. Chaney, "The Application of a Specific Detector for Phosphorous and for Sulfur Compounds - Sensitive to Nanogram Quantities", J. Gas Chromatog., 4, 42-46 (1966); P. J. Maroulis and A. R. Bandy, "Estimate of the Contribution of Biologically Produced Dimethyl Sulfur to the Global Sulfur Cycle", Science, 196, 647-648 (1977).
7. C. H. Moeller, II, K. Schofield, M. Steinberg and H. P. Broida, "Sulfur Chemistry in Flames", Seventeenth Symposium (International) on Combustion, Leeds, England, August 1978.
8. S. R. Leone and K. G. Kosnik, "A Tunable Visible Ultraviolet Laser on S_2 ($B^3\Sigma_u^- - X^3\Sigma_g^-$)", Appl. Phys. Lett., 30, 346-348 (1977).
9. K. A. Meyer and D. R. Crosley, "Franck-Condon Factors From Selectively Excited Resonance Fluorescence in the B-X System of S_2 ", J. Chem. Phys., 59, 3153-3161 (1973).
10. Such a correlation should be applied to the intensities of the rotationally resolved branches used to determine the intensity of the excitation term; however, this is a negligible amount. See K. A. Meyer and D. R. Crosley, "Rotational Satellite Intensities and Triplet Splitting in the $B^3\Sigma_u^-$ State of S_2 ", Can. J. Phys., 51, 2119-2124 (1973).

REFERENCES (Cont'd)

11. K. A. Meyer and D. R. Crosley, "Hanle Effect Lifetime Measurements on Selectively Excited Diatomic Sulfur", J. Chem. Phys., 59, 1933-1941 (1973).
12. G. D. Brabson, "Calculation of Morse Wave Functions with Programmable Desktop Calculators", J. Chem. Ed., 50, 397-399 (1973).
13. G. D. Brabson and R. L. Volkmar, "Calculation of Potential Energy Curves for S₂ Perturbed by a Frozen Inert Gas Matrix Environment", J. Chem. Phys., 58, 3209-3215 (1973).
14. To quote the late E. U. Condon, ["The Franck-Condon Principle and Related Topics", Amer. J. Phys., 15, 365-374 (1947)]: "The Franck-Condon patterns form real and forceful proof ... of the reality of de Broglie waves associated with the nuclear motions in the molecules". We thank Dr. R. N. Zare for drawing our attention to this delightful and instructive article.
15. G. Herzberg and L. G. Mundie, "On the Predissociation of Several Diatomic Molecules", J. Chem. Phys., 8, 263-273 (1940).

APPENDIX A

The laser excites the S_2 in the center of a T-shaped cell, so that the emitted radiation passes through a layer (~ 4 cm) of S_2 vapor before reaching the exit window. At higher pressures, some of the fluorescence for low v'' bands will be absorbed by this layer. This absorption coefficient for the i^{th} band is proportional to $q_i F_i p$, where F_i is the fraction of molecules in the i^{th} ground state vibrational level and p is the S_2 pressure. Consequently,

$$(I_i/I_j)_{\text{window}} = (I_i/I_j)_{\text{center}} \exp [-cp (q_i F_i - q_j F_j)] \quad .$$

The correction is made empirically, using measurements of the ratio of the intensity of each band of interest to the intensity of a band with high enough v'' that the level has negligible population. A plot of the logarithm of the ratio vs. p provides a straight line which is used to extrapolate the measured intensity to that which would be observed at zero pressure. Typical necessary corrections to the strongest bands are about 20 percent, with an estimated 20 percent error in the amount of correction. This uncertainty is included in the $\delta q_{v''}$ values where appropriate.

APPENDIX B

The analysis for the rotational quantum numbers of the excited level depends primarily on the splitting between the main R and P branches of the rotationally resolved fluorescence (See Fig. 4a). To a first approximation (that is, neglecting the triplet splitting), the separation $\Delta\nu_{RP} = 4B_{v'}(J' + 1/2)$. Using this value of J' and knowledge of the triplet component involved (see below), an improved value of J' is calculated taking into account the influence of the triplet splitting (see reference 1 of text).

The occurrence of rotational satellites is expected (see reference 12 of text) in fluorescence from F_1 or F_3 levels in $v' = 2, 6$, and 7 . The observation of a satellite may then be used to assign the triplet component involved, and the separation of the satellite from the nearest main branch provides further data on the value of J' . The results are summarized in the table where the columns labeled N' (main) and N' (satellite) list the quantum numbers obtained from the analysis of these respective splittings. Since only alternate rotational levels exist in the $B^3\Sigma_u^-$ state, the closest even value is used for the assignment.

There exists no prior information concerning the expectation of satellites (see reference 12 of text) in emission from $v' = 8$ or 9 . None is observed here. In the case of $v' = 9$, a value of $N' = 36$ was obtained from the R-P splitting. The excitation was by an R-branch in the $(9,0)$ band, measured to be at 35251 cm^{-1} . We compare this with a rotational analysis* yielding the values 32250 , 35237 , and 35241 cm^{-1} for $R_1(36)$, $R_2(36)$, and $R_3(36)$ respectively, to assign this excitation to the $F_1(36)$ level. Thus, $v' = 9$ does not have satellites and thus probably has a positive value of the triplet splitting parameter (see reference 12 of text). We do note that $F_1(36)$ is the highest bound level* in $v' = 9$ before the onset of predissociation. This could affect the presence or absence of satellite emission.

For $v' = 8$, we have no previous analysis which would yield a choice of triplet component. The excitation was $R(28)$ in the $(8,0)$ band, at 34858 cm^{-1} .

* J. M. Ricks and R. F. Barrow, "The Dissociation of Gaseous Diatomic Sulfur", *Can J. Phys.*, 47, 2423-2427 (1969).

SUMMARY OF RESULTS OF ROTATIONAL ANALYSIS

<u>v'</u>	<u>N' (main)</u>	<u>Observed Satellite</u>	<u>N' (Satellite)</u>	<u>Assignment</u>
2	46.0	$T_{R_{31}}$	43.9	$F_3(46)$
6	33.8	$N_{P_{13}}$	33.6	$F_1(34)$
7	30.4	$T_{R_{31}}$	27.5	$F_3(30)$
8	27.9	----	----	$N'=28$
9	35.7	----	----	$F_1(36)$

DISTRIBUTION LIST

<u>No. of</u> <u>Copies</u>	<u>Organization</u>	<u>No. of</u> <u>Copies</u>	<u>Organization</u>
12	Commander Defense Technical Info Center ATTN: DDC-DDA Cameron Station Alexandria, VA 22314	1	Commander US Army Armament Materiel Readiness Command ATTN: DRSAR-LEP-L, Tech Lib Rock Island, IL 61299
1	Director Defense Advanced Research Projects Agency ATTN: LTC C. Buck 1400 Wilson Boulevard Arlington, VA 22209	1	Director US Army ARRADCOM Benet Weapons Laboratory ATTN: DRDAR-LCB-TL Watervliet, NY 12189
2	Director Institute for Defense Analysis ATTN: H. Wolfhard R. T. Oliver 400 Army-Navy Drive Arlington, VA 22202	1	Commander US Army Watervliet Arsenal ATTN: Code SARWV-RD, R.Thierry Watervliet, NY 12189
1	Commander US Army Materiel Development and Readiness Command ATTN: DRCDMD-ST 5001 Eisenhower Avenue Alexandria, VA 22333	1	Commander US Army Aviation Research and Development Command ATTN: DRSARV-E P. O. Box 209 St. Louis, MO 63166
2	Commander US Army Armament Research and Development Command ATTN: DRDAR-TSS Dover, NJ 07801	1	Director US Army Air Mobility Research and Development Laboratory Ames Research Center Moffett Field, CA 94035
5	Commander US Army Armament Research and Development Command ATTN: DRDAR-LCA, J. Lannon DRDAR-LC, T.Vladimiroff DRDAR-LCE, F. Owens DRDAR-SCA, L. Stiefel DRDAR-LC, D. Downs Dover, NJ 07801	1	Commander US Army Communications Rsch and Development Command ATTN: DRDCO-PPA-SA Fort Monmouth, NJ 07703
		1	Commander US Army Electronics Research and Development Command Technical Support Activity ATTN: DELSD-L Fort Monmouth, NJ 07703

DISTRIBUTION LIST

<u>No. of</u> <u>Copies</u>	<u>Organization</u>	<u>No. of</u> <u>Copies</u>	<u>Organization</u>
1	Commander US Army Missile Command ATTN: DRSMI-R Redstone Arsenal, AL 35809	1	Director US Army TRADOC Systems Analysis Activity ATTN: ATAA-SL, Tech Lib White Sands Missile Range NM 88002
1	Commander US Army Missile Command ATTN: DRSMI-YDL Redstone Arsenal, AL 35809	2	Office of Naval Research ATTN: Code 473 G. Neece 800 N. Quincy Street Arlington, VA 22217
1	Commander US Army Natick Research and Development Command ATTN: DRXRE, D. Sieling Natick, MA 01762	1	Commander Naval Sea Systems Command ATTN: J.W. Murrin, SEA-62R2 National Center Bldg. 2, Room 6E08 Washington, DC 20360
1	Commander US Army Tank Automotive Research & Development Cmd ATTN: DRDTA-UL Warren, MI 48090	1	Commander Naval Surface Weapons Center ATTN: Library Br., DX-21 Dahlgren, VA 22448
1	Commander US Army White Sands Missile Range ATTN: STEWS-VT White Sands, NM 88002	2	Commander Naval Surface Weapons Center ATTN: S. J. Jacobs, Code 240 Code 730 Silver Spring, MD 20910
1	Commander US Army Materials and Mechanics Research Center ATTN: DRXMR-ATL Watertown, MA 02172	1	Commander Naval Underwater Systems Cmd Energy Conversion Department ATTN: R.S. Lazar, Code 5B331 Newport, RI 02840
3	Commander US Army Research Office ATTN: Tech Lib D. Squire F. Schmiedeshaff R. Ghirardelli M. Ciftan P. O. Box 12211 Research Triangle Park NC 27706	2	Commander Naval Weapons Center ATTN: R. Derr C. Thelen China Lake, CA 93555

DISTRIBUTION LIST

<u>No. of</u> <u>Copies</u>	<u>Organization</u>	<u>No. of</u> <u>Copies</u>	<u>Organization</u>
1	Commander Naval Research Laboratory ATTN: Code 6180 Washington, DC 20375	1	Atlantic Research Corporation ATTN: M. K. King 5390 Cherokee Avenue Alexandria, VA 22314
3	Superintendent Naval Postgraduate School ATTN: Tech Lib D. Netzer A. Fuhs Monterey, CA 93940	1	AVCO Corporation AVCO Everett Research Lab Div ATTN: D. Stickler 2385 Revere Beach Parkway Everett, MA 02149
2	Commander Naval Ordnance Station ATTN: A. Roberts Tech Lib Indian Head, MD 20640	1	Foster Miller Associates, Inc. ATTN: A. J. Erickson 135 Second Avenue Waltham, MA 02154
3	AFOSR (B.T. Wolfson; D. Ball; L. Caveny) Bolling AFB, DC 20332	1	General Electric Company Armament Department ATTN: M. J. Bulman Lakeside Avenue Burlington, VT 05402
2	AFRPL (DYSC) - ATTN: D. George J. N. Levine Edwards AFB, CA 93523	1	General Electric Company Flight Propulsion Division ATTN: Tech Lib Cincinnati, OH 45215
2	National Bureau of Standards ATTN: J. Hastie T. Kashiwagi Washington, DC 20234	2	Hercules Incorporated Alleghany Ballistic Lab ATTN: R. Miller Tech Lib Cumberland, MD 21501
1	Lockheed Palo Alto Rsch Labs ATTN: Tech Info Ctr 3521 Hanover Street Palo Alto, CA 94304	1	Hercules Incorporated Bacchus Works ATTN: B. Isom Magna, UT 84044
1	Aerojet Solid Propulsion Co. ATTN: P. Micheli Sacramento, CA 95813	1	IITRI ATTN: M. J. Klein 10 West 35th Street Chicago, IL 60615
1	ARO Incorporated ATTN: N. Dougherty Arnold AFS, TN 37389		

DISTRIBUTION LIST

<u>No. of Copies</u>	<u>Organization</u>	<u>No. of Copies</u>	<u>Organization</u>
1	Olin Corporation Badger Army Ammunition Plant ATTN: J. Ramnarace Baraboo, WI 53913	1	Shock Hydrodynamics, Inc. ATTN: W. H. Anderson 4710-16 Vineland Avenue North Hollywood, CA 91602
2	Olin Corporation New Haven Plant ATTN: R.L. Cook D.W. Riefler 275 Winchester Avenue New Haven, CT 06504	1	Thiokol Corporation Elkton Division ATTN: E. Sutton Elkton, MD 21921
1	Paul Gough Associates, Inc. ATTN: P.S. Gough P. O. Box 1614 Portsmouth, NH 03801	3	Thiokol Corporation Huntsville Division ATTN: D. Flanigan R. Glick Tech Lib Huntsville, AL 35807
1	Physics International Co. 2700 Merced Street Leandro, CA 94577	2	Thiokol Corporation Wasatch Division ATTN: J. Peterson Tech Lib P. O. Box 524 Brigham City, UT 84302
1	Pulsepower Systems, Inc. ATTN: L. C. Elmore 815 American Street San Carlos, CA 94070	1	TRW Systems Group ATTN: H. Korman One Space Park Redondo Beach, CA 90278
3	Rockwell International Corp. Rocketdyne Division ATTN: C. Obert J. E. Flanagan A. Axeworthy 6633 Canoga Avenue Canoga Park, CA 91304	2	United Technology Center ATTN: R. Brown Tech Lib P. O. Box 358 Sunnyvale, CA 94088
2	Rockwell International Corp. Rocketdyne Division ATTN: W. Haymes Tech Lib McGregor, TX 76657	1	Universal Propulsion Co. ATTN: H.J. McSpadden 1800 W. Deer Valley Road Phoenix, AZ 85027
1	Science Applications, Inc. ATTN: R. B. Edelman Combustion Dynamics and Propulsion Division 23146 Cumorah Crest Woodland Hills, CA 91364	11	Battelle Memorial Institute ATTN: Tech Lib R. Bartlett (10 cys) 505 King Avenue Columbus, OH 43201

DISTRIBUTION LIST

<u>No. of Copies</u>	<u>Organization</u>	<u>No. of Copies</u>	<u>Organization</u>
1	Brigham Young University Dept of Chemical Engineering ATTN: M. W. Beckstead Provo, UT 84601	1	Pennsylvania State University Dept of Mechanical Engineering ATTN: K. Kuo University Park, PA 16801
1	California Institute of Tech 204 Karmar Lab Mail Stop 301-46 ATTN: F.E.C. Culick 1201 E. California Street Pasadena, CA 91125	1	Pennsylvania State University Dept of Material Sciences ATTN: H. Palmer University Park, PA 16801
1	Case Western Reserve Univ. Division of Aerospace Sciences ATTN: J. Tien Cleveland, OH 44135	2	Princeton University Forrestal Campus ATTN: I. Glassman Tech Lib P. O. Box 710 Princeton, NJ 08540
3	Georgia Institute of Tech School of Aerospace Eng. ATTN: B. T. Zinn E. Price W.C. Strahle Atlanta, GA 30332	2	Purdue University School of Mechanical Eng ATTN: J. Osborn S.N.B. Murthy TSPC Chaffee Hall West Lafayette, IN 47906
1	Institute of Gas Technology ATTN: D. Gidaspow 3424 S. State Street Chicago, IL 60616	1	Rutgers State University Dept of Mechanical and Aerospace Engineering ATTN: S. Temkin University Heights Campus New Brunswick, NJ 08903
1	Johns Hopkins University/APL Chemical Propulsion Info Agency ATTN: T. Christian Johns Hopkins Road Laurel, MD 20810	4	SRI International ATTN: Tech Lib D. Crosley J. Barker D. Golden 333 Ravenswood Avenue Menlo Park, CA 94025
1	Massachusetts Inst of Tech Dept of Mechanical Engineering ATTN: T. Toong Cambridge, MA 02139	1	Stevens Institute of Tech Davidson Library ATTN: R. McAlevy, III Hoboken, NJ 07030
1	Pennsylvania State University Applied Research Lab ATTN: G. M. Faeth P. O. Box 30 State College, PA 16801		

DISTRIBUTION LIST

<u>No. of Copies</u>	<u>Organization</u>
1	University of California, San Diego Ames Department ATTN: F. Williams P. O. Box 109 La Jolla, CA 92037
1	University of Illinois Dept of Aeronautical Eng ATTN: H. Krier Transportation Bldg, Rm 105 Urbana, IL 61801
1	University of Minnesota Dept of Mechanical Eng. ATTN: E. Fletcher Minneapolis, MN 55455
1	University of Southern California Department of Chemistry ATTN: S. Benson Los Angeles, CA 90007
1	University of Texas Dept of Chemistry ATTN: W. Gardiner H. Schaefer Austin, TX 78712
2	University of Utah Dept of Chemical Engineering ATTN: A. Baer G. Flandro Salt Lake City, UT 84112
<u>Aberdeen Proving Ground</u>	
	Dir, USAMSAA ATTN: DRXSY-D DRXSY-MP, H. Cohen Cdr, USATECOM ATTN: DRSTE-TO-F Dir, USA CSL, Bldg. E3516 ATTN: DRDAR-CLB-PA

USER EVALUATION OF REPORT

Please take a few minutes to answer the questions below; tear out this sheet and return it to Director, US Army Ballistic Research Laboratory, ARRADCOM, ATTN: DRDAR-TSB, Aberdeen Proving Ground, Maryland 21005. Your comments will provide us with information for improving future reports.

1. BRL Report Number _____

2. Does this report satisfy a need? (Comment on purpose, related project, or other area of interest for which report will be used.)

3. How, specifically, is the report being used? (Information source, design data or procedure, management procedure, source of ideas, etc.) _____

4. Has the information in this report led to any quantitative savings as far as man-hours/contract dollars saved, operating costs avoided, efficiencies achieved, etc.? If so, please elaborate.

5. General Comments (Indicate what you think should be changed to make this report and future reports of this type more responsive to your needs, more usable, improve readability, etc.) _____

6. If you would like to be contacted by the personnel who prepared this report to raise specific questions or discuss the topic, please fill in the following information.

Name: _____

Telephone Number: _____

Organization Address: _____

